



HAL
open science

A new framework for solving en-routes conflicts

Cyril Allignol, Nicolas Barnier, Nicolas Durand, Jean-Marc Alliot

► **To cite this version:**

Cyril Allignol, Nicolas Barnier, Nicolas Durand, Jean-Marc Alliot. A new framework for solving en-routes conflicts. ATM 2013, 10th USA/Europe Air Traffic Management Research and Development Seminar, Jun 2013, Chicago, United States. pp 1-9. hal-00828736

HAL Id: hal-00828736

<https://hal-enac.archives-ouvertes.fr/hal-00828736>

Submitted on 31 May 2013

HAL is a multi-disciplinary open access archive for the deposit and dissemination of scientific research documents, whether they are published or not. The documents may come from teaching and research institutions in France or abroad, or from public or private research centers.

L'archive ouverte pluridisciplinaire **HAL**, est destinée au dépôt et à la diffusion de documents scientifiques de niveau recherche, publiés ou non, émanant des établissements d'enseignement et de recherche français ou étrangers, des laboratoires publics ou privés.

A New Framework for Solving En-Route Conflicts

Cyril Allignol, Nicolas Barnier, Nicolas Durand

ENAC/MAIAA
7 av. Édouard Belin
31055 Toulouse Cedex, France
allignol,barnier,durand@recherche.enac.fr

Jean-Marc Alliot

IRIT – Université Paul Sabatier
118 Route de Narbonne
31062 Toulouse, France
jean-marc.alliot@aviation-civile.gouv.fr

Abstract—The en-route conflict resolution problem has been modeled in many different ways, generally depending on the tools that were proposed to solve it. For instance, with purely analytic mathematical solvers, models tend to be very restrictive (constant speeds, linear trajectories...) to respect the inherent limitations of the technology.

This paper introduces a new framework that separates the model from the solver so as to be able to: first, enhance the model with as many refinements (e.g. wind and trajectory uncertainties) as necessary to comply with operational constraints; second, compare different resolution methods on the same data, which is one of the crucial aspects of scientific research.

To this aim, our framework can generate a benchmark of conflict resolution problems built with various scenarios involving a given number of aircraft, level of uncertainties and number of maneuvers. We then compare two different optimization paradigms, Evolutionary Algorithm and Constraint Programming, which can efficiently solve difficult instances in near real time, to illustrate the usefulness of our approach.

Keywords: conflict resolution, evolutionary computation, constraint programming

I. INTRODUCTION

An effective conflict solver relies on a realistic trajectory prediction. Today, because of different uncertainty sources (e.g. wind and aircraft mass), air traffic management systems are not able to predict the future positions of aircraft with a good accuracy and must take into account all these uncertainties to choose the best trajectories in terms, first, of safety and then efficiency. This probably explains why the short term traffic resolution system still relies on human expertise and is not automated yet.

A lot of research has been done on conflict detection and resolution and many papers present models that are so impractical that they strengthen the readers' beliefs that automating the conflict detection and resolution task is not realistic in the near future. For example, the approach using repulsive forces described in [1] or the B-spline approximation model of [2] are very interesting on a mathematical level but could hardly be implemented in an operational context. They suppose continuous heading changes, which Flight Management Systems (FMS) are unable to exploit, and do not take uncertainties into account. Pallottino's approach [3] using mixed integer linear programming (as [4], [5], [6]) relies on constant speed trajectories that are changed all at once. None

of these approaches could deal with realistic trajectory models able to handle evolutive aircraft or trajectory uncertainties.

Other approaches have been proposed, with more realistic models, like [7], [8] which use the Base of Aircraft Data (BADA) developed and maintained by EUROCONTROL in CATS (Complete Air Traffic Simulator) to solve conflicts using Evolutionary Algorithms. This model introduces uncertainties on aircraft speed, climb and descent rate, thus the solver needs to compute many alternative trajectories in real time. Nevertheless, the solver is quite efficient as it can handle complete days of traffic in the European airspace. However, these algorithms are difficult to compare with other methods because the conflict detection is embedded in the solver. This problem also occurs in Erzberger's approach [9], where most of the expertise is focused on the trajectory and maneuver model. But once more, the presented results can hardly be compared with other algorithms because the resolution maneuver generator is embedded in the solver.

In this paper, we propose a new framework to deal with conflict resolution, which, from a given scenario, computes a 4D-matrix indexed by aircraft pairs and maneuvers (i.e. trajectories) pairs that provides all the necessary data to solve the problem. Hence, the detection and maneuver model is separated from the resolution, which enables to compare the behavior of various algorithms on the same instances. As the conflict resolution problem is highly combinatorial [10] and as large instances can therefore be very difficult to optimize, it is of utmost importance to be able to assess the relative merits of solvers, even if finding the optimal solution is often not required in a real-time context (a "good" conflict-free solution can be sufficient).

In our benchmark framework, finding the future positions can be done using any simulator and can take into account different uncertainty sources such as wind, heading change, beginning and ending maneuver positions, etc. Once the future positions for every possible maneuvers are found, a simple algorithm can detect conflicts for each pair of aircraft and store this information in a 4D conflict matrix C , the first two indexes specifying the pair of aircraft involved and the next two the concerned maneuvers. For example, $C_{i,j,k,l}$ returns *true* if maneuver k of aircraft i and maneuver l of aircraft j are conflicting, and *false* otherwise. When solving conflicts, instead of recomputing the trajectory positions of each aircraft, solvers can refer to this 4D-matrix very fast, in constant time

complexity.

We then illustrate how resolution times and costs of different solvers can be fairly compared within our benchmark framework. Two resolution algorithms using different optimization paradigms have been implemented: a metaheuristic, namely an Evolutionary Algorithm [11], which is able to handle over-constrained or very large instances, but cannot provide optimality proofs, and a Constraint Program [12], which has the converse properties (may be stalled while backtracking for large scale problems, but able to provide proofs of optimality or absence of solution for reasonable ones).

The next section of this paper introduces the model that was chosen to build the trajectories of our benchmark framework. We particularly detail its uncertainty model and how the convex hulls of trajectories are built. Section III describes the method used to build conflicting scenarios with different sizes (number of aircraft) and levels of uncertainties, before presenting the detection algorithm that builds the 4D conflict matrix. We then detail in section IV two approaches for the resolution of conflicts, an Evolutionary Algorithm and a Constraint Program, to illustrate their comparison with our benchmark framework in section V, where some experimental results are analyzed.

II. TRAJECTORY PREDICTION MODEL

In this paper, we give an example of a trajectory prediction tool that can be used to build the aircraft positions at each time step according to the chosen maneuver options and the uncertainties taken into account. To constrain the search space to a “reasonable” size, only a limited number of maneuvers, compatible with current ATC practice and FMS capabilities, is defined for each aircraft involved in a conflict. Then each pair of maneuvers for two different aircraft are tested to check if they are conflicting or not.

Moreover, our model is able to handle various degrees of uncertainties by considering the future positions of aircraft not simply as mere 2D-points in the airspace but as growing convex envelopes representing all its possible positions. Loss of separation between aircraft are then detected by computing the minimal distance between their two envelopes.

A. Maneuvers

In our trajectory prediction model, a discretization of time into steps of duration τ is used to describe maneuvers. τ is chosen small enough to detect every conflict in the application. For example, in section III-A, $\tau = 3$ s because two facing aircraft flying at 600 kt (maximal speed) get only 1 NM closer every 3 s, so no conflict could be missed with such a small τ value (see [13] for a discussion on this topic).

Trajectories are defined in the horizontal plane, but the scenarios could be easily extended to the vertical dimension if we used a proper flight simulator. Initial routes are defined by a list of points. The first point O is the origin and the last point D is the destination (e.g. a segment of trajectory between two waypoints). Aircraft fly from point to point and are able to correct the lateral error to the original trajectory

thanks to their FMS. This means that in the further examples, the associated uncertainty does not increase with time.

However, various other sources of uncertainties cannot be reduced by current FMS features and must be taken into account in our model. Aircraft speeds are hence subject to a ε_s error such that future positions of aircraft are spread over a range which grows with time.

In our trajectory model, maneuvers (i.e. heading changes) are engaged on a point of the initial trajectory referenced by the decision variable d_0 , which represents the curvilinear distance from the origin O . Because of uncertainties on the exact location of the turn, a distance error ε_0 is added around this point. This means that the aircraft may start the maneuver ε_0 nautical miles before or after d_0 .

An uncertainty ε_α is also associated to the heading change angle α at the turning point corresponding to d_0 . Then the maneuver ends at a curvilinear distance d_1 from d_0 (i.e. at $d_0 + d_1$ from the origin O) with an associated error ε_1 , when the aircraft returns towards its destination point D .

This kind of simple maneuvers, depicted in figure 1, are representative of current Air Traffic Control practice and can be easily implemented by pilots and current FMS technologies (cf. [8]), unlike continuous maneuvers at arbitrary angles and distances that are used in many conflict resolution models [1], [2].

In order to limit the number of maneuvers created, and thus the size of the search space, d_0 can only take a limited number n_0 of values (typically $n_0 = 5$ in the experimental benchmark presented in section V). The heading change α can also take $n_\alpha = 7$ different values in our benchmark, i.e. 0, 10, 20 or 30 degrees to the left or the right of the current heading, and the number of values for the distance of the returning point d_1 is also limited by n_1 (typically $n_1 = 5$).

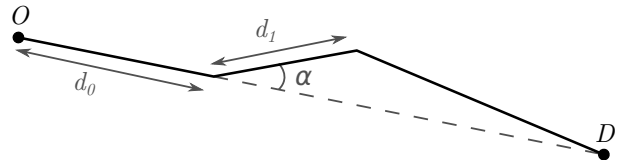


Fig. 1. Maneuver model.

If we consider 5 values for d_0 , 5 values for d_1 and the 6 possible angles (there is no use to combine a null heading change $\alpha = 0$ with various d_0 and d_1 values, so that only one maneuver is added when the aircraft is not deviated), the number of maneuvers per aircraft is:

$$n_{\text{man}} = n_0 \times n_1 \times (n_\alpha - 1) + 1$$

So for the benchmark presented in section III-A: $n_{\text{man}} = 5 \times 5 \times 6 + 1 = 151$.

For an instance with n aircraft, the search space is then of size n_{man}^n , i.e. $\approx 6.10^{21}$ for a 10-aircraft instance (almost 4.10^{43} for 20 aircraft).

B. Decision Variables

To simplify the access to the conflict matrix C and reduce the number of combinations to the useful ones (e.g. only one

possible maneuver for $\alpha = 0$), the three decision variables d_0 , α and d_1 associated with aircraft i are aggregated into a single decision variable m_i by a bijection from the allowed triples to interval $[1, n_{\text{man}}]$. We call M the set of decision variables of the problem:

$$M = \{m_i, i \in [1, n]\} \quad (1)$$

C. Cost

The maneuver cost of our model is straightforwardly computed from the decision variables. Values of d_0 are enumerated by an index k_0 varying in $[1, n_0]$, values of d_1 by index k_1 in $[1, n_1]$ and angles α of value 10, 20 or 30 degrees right or left, are respectively indexed by k_α in $[1, \frac{n_\alpha}{2}]$. For our benchmark problems, the cost of a maneuver m_i for aircraft i is then defined as follows:

$$\text{cost}_{\text{man}}(m_i) = \begin{cases} 0 & \text{if } \alpha = 0 \\ (n_0 - k_0)^2 + k_1^2 + k_\alpha^2 & \text{otherwise} \end{cases} \quad (2)$$

where k_0 , k_1 and k_α are the indexes corresponding to maneuver m_i . This cost is null whenever an aircraft is not maneuvered.

Furthermore, this cost function ensures the following properties:

- 1) any maneuver is more costly than no maneuver;
- 2) maneuvers should start as late as possible;
- 3) maneuvers should be as short as possible;
- 4) the angle should be as small as possible.

In a real environment, the cost function should be adapted to the aircraft performance model or to other criteria, including controllers' preferences and fuel consumption. However, this paper aims at giving a framework that dissociates the solver method from the problem itself, so as to provide the scientific community (which may be unfamiliar with ATM and conflict resolution) with the simplest possible framework which enables to compare different solvers on our benchmark.

Given an instance with n aircraft, we define the cost of a solution as the sum of the maneuvers costs:

$$\text{cost} = \sum_{i=1}^n \text{cost}_{\text{man}}(m_i) \quad (3)$$

D. Handling Uncertainties

We shall now describe how the trajectories envelopes are build in order to be able to detect conflicts between two maneuvers for two different aircraft, while taking various uncertainties into account.

In our framework, the maneuvers description are stored in a table that defines for each aircraft and each maneuver the possible future positions of the aircraft at every time step. These positions are represented by their convex hull, which is computed with Graham's algorithm [14].

Each aircraft position is described at multiples of the time step τ (i.e. $0, \tau, 2\tau, 3\tau \dots$) by three convex hulls corresponding to the three possible states of the aircraft:

- S_0 if it has not been maneuvered yet;
- S_1 if it is currently maneuvered;

- S_2 if it is heading towards its destination after a maneuver.

Once the three convex hulls are defined for every time step, they are merged in a single one whenever several envelopes coexist for the same time step (e.g. around turning points of the trajectory).

We first start with one point representing the current position of the aircraft at $t = 0$. To build the possible positions at $t + \tau$, we take into account every extreme position of the three convex hulls at time t and calculate the future possible positions of each point. During this process, some points stay in the same state while others change near the turning points of the trajectory. Moreover, some points may generate two different future positions in two different states. For example, a point in state S_0 (before any maneuver) may reach $d_0 - \varepsilon_0$ at the next step if the aircraft flies at the fastest possible speed according to the amount of uncertainty taken into account by parameter ε_0 . It will then change heading and be in state S_1 . The same point may as well fly at the lowest possible speed and stay in state S_0 . After each movement, the convex hull of the cloud of points created is computed for each state. At the very end of the process, the convex hull of the whole trajectory is calculated for each time step.

Figure 2 gives an example of maneuver with the different states. In red, the aircraft has not start any maneuver. In green, the aircraft has changed its heading, and in blue, it is heading back to the next point on its route (D). The gray line gives the convex hull of the three states. The conflicts will then be detected among such envelopes by computing their minimal distance.

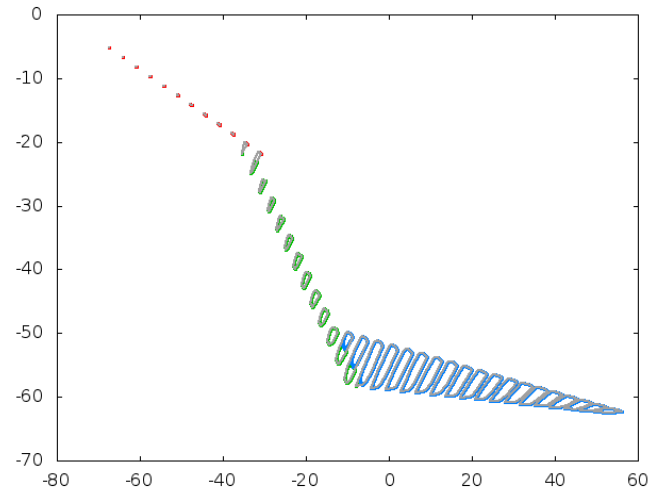


Fig. 2. An example of trajectory prediction. Red, green and blue correspond respectively to states S_0 , S_1 and S_2 ; gray parts represent the convex hulls.

It is important to notice that any traffic simulator using any kind of uncertainty hypothesis could be used to build the trajectory prediction for the aircraft and for the maneuver options. Different aircraft could have different uncertainties and different maneuver options according to their ability to follow a route. We only need a convex hull of the possible future positions of an aircraft at every time step of the trajectory.

This approach can easily be generalized to the third dimension (vertical plane), taking into account uncertainties on the climbing rate of the aircraft. Convex 3D-volumes would thus be defined and conflicts detected according to the distance between them.

III. BENCHMARK GENERATION

The trajectory prediction presented in the previous section is used to produce the data for the proposed benchmark. To generate an instance, two consecutive processes are involved: first the creation of conflicting scenarios, presented in section III-A, then the detection of conflicts, detailed in section III-B.

A. Scenarios

In the experimental results presented in section V, instances of four different sizes have been considered, involving $n = 5, 10, 15$ and 20 aircraft, with three levels of uncertainties. For each combination, 10 scenarios of aircraft converging to the center of the considered airspace volume were randomly built. For each scenario, speeds are chosen from 384 kt to 576 kt (i.e. 20% variation around a typical speed of 480 kt). The aircraft initial positions are chosen on a 70 NM radius circle and are noised within a 20 NM-side square. The initial heading is also noised with a value chosen in $[-1, 1]$ radians ($\approx \pm 60^\circ$). Figure 3 illustrates this geometry on an instance with 4 aircraft.

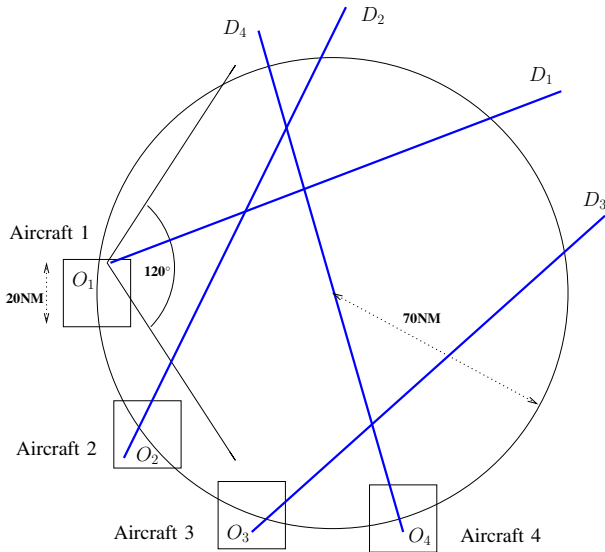


Fig. 3. Geometry of the conflict scenario generation (with 4 aircraft).

A total of 40 scenarios were built to compare the algorithms. For each scenario, three levels of uncertainty are defined. The lower level of uncertainty ε_{low} takes into account $\varepsilon_s = 1\%$ of error on the aircraft speed, $\varepsilon_0 = 1$ NM of error on the location of the turning point, $\varepsilon_\alpha = 1^\circ$ on the angle of the turn and $\varepsilon_1 = 1$ NM of error on the location of the returning point. The medium level of uncertainty ε_{med} doubles every value: $\varepsilon_s = 2\%$, $\varepsilon_0 = 2$ NM, $\varepsilon_\alpha = 2^\circ$ and $\varepsilon_1 = 2$ NM. Finally, the higher level of uncertainty $\varepsilon_{\text{high}}$ triples the lower uncertainty values: $\varepsilon_s = 3\%$, $\varepsilon_0 = 3$ NM, $\varepsilon_\alpha = 3^\circ$ and $\varepsilon_1 = 3$ NM.

120 scenarios are thus built as a proposed benchmark basis and we next detail how conflict are detected to complete the framework description.

B. Conflict Detection

Once the trajectory predictions computed and stored, the 4D conflict matrix C can be built. To simplify the access to the matrix and reduce the number of combinations to the useful ones (e.g. only one possible maneuver for $\alpha = 0$), the three decision variables d_0 , α and d_1 are aggregated in a single decision variable by a bijection from the allowed triples to interval $[1, n_{\text{man}}]$. Then, for each pair of aircraft (i, j) and each pair of maneuver options (k, l) (where k is a maneuver option for aircraft i and l for aircraft j), we test if maneuvers k and l generate a conflict. In this case, $C_{i,j,k,l} = 1$ (i.e. *true*), otherwise $C_{i,j,k,l} = 0$ (i.e. *false*). Furthermore, the matrix is symmetric along its two first dimensions, since a conflict between i and j is equivalent to a conflict between j and i , so we only consider pairs of aircraft such that $i < j$.

To detect a conflict, the distance between the two envelopes representing the possible positions of aircraft i and j is computed and compared to the standard separation norm (5 NM). For every time step, the algorithm is divided in three stages:

- 1) Check if a vertex of convex hull k is inside convex hull l , or if a vertex of convex hull l is inside convex hull k .
- 2) Otherwise, check if two edges of convex hulls k and l intersect.
- 3) Otherwise, check the distance between every vertex of convex hull k and every edge of convex hull l , or every vertex of convex hull l with every edge of convex hull k . As soon as one of the distances is smaller than the separation standard, $C_{i,j,k,l}$ is set to 1.

This calculation is the most time consuming of the problem generation because the number of pairs tested is big. For example, a 20-aircraft conflict with 151 maneuvers per aircraft generates $\frac{20 \times 19}{2} = 190$ pairs of aircraft for which $151^2 = 22,801$ pair of maneuvers must be tested. A total of 4,332,190 pairs of maneuvers must be tested to build the conflict matrix.

However, this operation can be parallelized very easily. For instance, different processors can be used to test different pairs of maneuvers. The computation time can thus drastically be reduced. We give different examples in section V of the time required to compute $C_{i,j,k,l}$ as a function of the number of processors. Furthermore, sweep-line techniques [15] could be used to lower the time complexity of the edge intersection checks performed during the second step of our convex hull distance algorithm. Eventually, a preliminary filtering by approximating the envelopes with simple enclosing boxes can spare many convex hull intersection checks.

Now that our framework is equipped with all the necessary pre-computed data needed to implement a conflict solver independently of the trajectory generation or the conflict detection, we describe in section IV two different approaches to solve the conflict scenarios of the proposed benchmark.

IV. CONFLICT RESOLUTION

In this section, we propose two methods for the resolution of the conflict scenarios generated with our benchmark framework. The first one, an Evolutionary Algorithm (section IV-A), is a metaheuristic that mimics natural evolution to explore the search space. The second one, Constraint Programming (section IV-B), is based on an efficient systematic search of the solution space, which enables to prove the optimality (or the absence) of a solution.

A. Evolutionary Algorithm

1) *Principles*: Our Evolutionary Algorithm (EA), described in algorithm 1, follows classical Evolutionary Computation principles such as presented in [16], [11].

Algorithm 1 Evolutionary algorithm (EA)

- 1: Initialize population
 - 2: **while** termination criterion is not met **do**
 - 3: Evaluate *raw fitness* of population elements
 - 4: Apply *scaling* and *sharing* operations on *raw fitness*
 - 5: Select new population w.r.t. *new fitness* criterion
 - 6: Replace some elements by *mutation* and *crossover*
 - 7: **end while**
 - 8: Return best elements of population
-

First, a population of points in the state space is randomly generated. Then, we compute for each population element the value of the function to optimize, which is called *fitness*. In a second step, we select¹ the best individuals in the population according to their fitness. Afterwards, we randomly apply classical evolutionary operators, i.e. *crossover* and *mutation*, to diversify the population (they are applied with respective probabilities P_c and P_m). At this step a new population has been created and we apply the process again in an iterative way.

2) *Sharing Improvement*: Our problem is very combinatorial and may have many different optimal solutions. In order to find most of these solutions² and to avoid local optima, the *sharing* process introduced by Yin and Gernay [17] is used. This improvement can be efficiently computed in $\Theta(p \log p)$ time complexity (instead of $\Theta(p^2)$ for the classical sharing process), where p is the size of the population.

A sharing process requires the definition of a distance between two chromosomes (two trajectory sets) to group alike population elements in the same *cluster*, according to a threshold parameter controlling the size and number of clusters. For the sake of simplicity, the distance implemented in our EA returns only two values: *true* if the elements (set of trajectories) are identical and *false* otherwise. The fitness of elements belonging to the same cluster is then divided

¹Selection aims at reproducing better individuals according to their fitness. We tried two kinds of selection process, "Roulette Wheel Selection" and "Stochastic Remainder Without Replacement Selection" (described in [16] for example); the latter always works out better.

²Finding several solutions is very interesting because the controller may choose among several options or negotiate them with pilots, keeping controllers and pilots alike in the decision making process.

by the size of the cluster to avoid an over-representation of a particular solution in the population and encourage diversification.

3) *Fitness Function*: The fitness function of our EA is very basic and does not aim at taking into account fuel consumption or controllers' preferences. We just focus on finding a conflict-free set of heading changes starting as late as possible, with the smallest deviation length and heading change.

The fitness function is then defined by two cases, depending on the presence (first case) or absence (second case) of remaining conflicts in the solution:

$$F = \begin{cases} \frac{1}{2 + \sum_{i < j} C_{i,j,m_i,m_j}} & \text{if } \exists(i,j), i < j, C_{i,j,m_i,m_j} \neq 0 \\ \frac{1}{2} + \frac{1}{1 + \text{cost}} & \text{if } \forall(i,j), i < j, C_{i,j,m_i,m_j} = 0 \end{cases}$$

where *cost*, defined by equation 3 in section II-C, represents the cost of a solution.

Moreover, this fitness function guarantees that if a chromosome value is larger than $\frac{1}{2}$, no conflict occurs, such that the cost of proper solutions is strictly greater than the cost of conflicting ones. If a conflict remains, the fitness does not take into account the cost of the maneuvers, allowing the EA to focus the search for conflict-free solutions first, regardless of the quality of the maneuvers involved.

4) *Adapted Crossover and Mutation*: EAs are very versatile because they do not require much information on the objective function. However, non-specific classical operators used by Gruber, Alliot and Schoenauer in [18] did not produce satisfactory results on our benchmark.

Nonetheless, in the case of the conflict resolution problem, we do know many properties about the fitness function, and they can be very useful to create adapted crossover and mutation operators. Durand, Alliot and Noailles describe such operators in [19].

The crossover operator, tailored to benefit from the structure of functions defined as a sum of positive terms, is described on figure 4. After choosing two parents A and B , we compare the number of conflicts remaining for both sets of maneuvers and choose the maneuver from the parent having the smallest number of conflicts. When both maneuvers generate the same number of conflicts, we pick up randomly the maneuver from parent A and parent B .

The mutation operator is described on figure 5. After choosing a chromosome, an aircraft is mutated (on figure 5, aircraft 4 is chosen). Maneuvers generating conflicts for the parent are chosen in priority and changed to favor conflict-free maneuvers in the offspring.

These operators are more deterministic at the beginning of the optimization, when many conflicts remain in the population, so that a solution without conflict can be found very quickly. When conflict-free solutions become sufficiently numerous, more randomness is allowed and other parts of the search space can be explored.

B. Constraint Programming

Constraint Programming (CP) is a versatile optimization technology based on the Constraint Satisfaction Problem

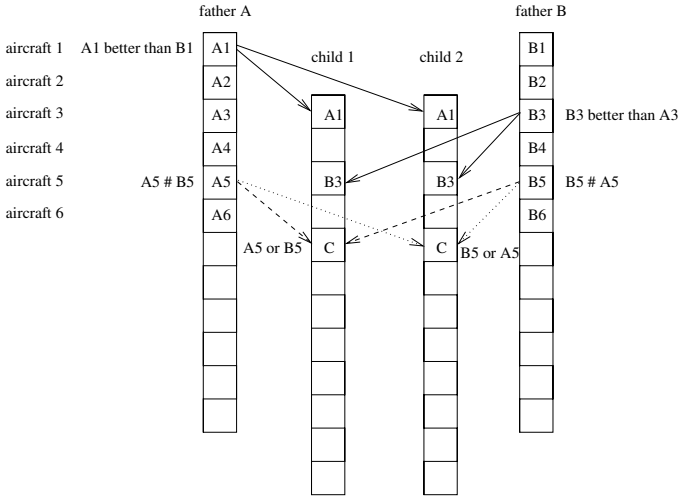


Fig. 4. Adapted crossover operator.

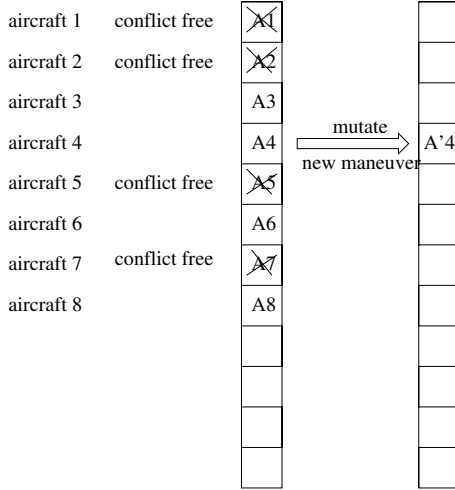


Fig. 5. Adapted mutation operator.

(CSP) formalism which emphasizes the satisfaction of combinatorial *constraints* (i.e. arbitrary relations over a set of decision variables). CP offers a clean separation between the modeling language and the resolution algorithms, enabling to quickly develop solvers in an incremental fashion and to experiment with various search strategies without changing the model. See [12] for example, where more details on the CP technology can be found.

1) *CSP Model*: The set M of decision variables of the CSP is the one defined by equation 1 in section II, where each variable m_i is the index of the maneuver for aircraft i and thus takes a value in $[1, n_{\text{man}}]$.

The constraints are expressed as *binary constraints*, i.e. constraints involving exactly two variables. For a given couple of aircraft i and j ($i < j$), the constraint c_{ij} between variables m_i and m_j is defined as the set:

$$c_{ij} = \{(m_i^k, m_j^l) \text{ s.t. } C_{i,j,k,l} = 1\} \quad (4)$$

where m_i^k and m_j^l are respectively the k -th and the l -th value of interval $[1, n_{\text{man}}]$ of the maneuvers available for aircraft i and j . c_{ij} therefore describes all couples of maneuvers that

cannot be performed by aircraft i and j without resulting in a conflict.

We denote by $|c_{ij}|$ the cardinal of the constraint c_{ij} , i.e. the number of forbidden couples of maneuvers.

2) *Solution Search*: The exploration of the search space is based on an enhanced version of a systematic tree-search algorithm called *backtracking*, where an inference phase prunes the unfeasible values of each variable at every node of the tree by propagating local consistency properties in the constraint network. In our algorithm, the search tree is explored by following the *weighted degree* [20] adaptive heuristic which learns from the failures during the search, so that the variables involved in the constraints that have been violated the most so far are instantiated first. This heuristic proved to be particularly efficient on this problem, as it dynamically focuses on the hardest parts of the CSP first.

3) *Optimization*: The optimization criterion c simply is the sum of the costs of each single maneuver as defined in equation 3 of section II-C. The optimization algorithm used to solve the CSP is an adaptation of the backtracking algorithm called *branch and bound*: each time a solution with cost c_s is found, the constraint $c < c_s$ is dynamically added to the CP model, and the search is resumed to look for a better solution. Eventually, the search for a better solution will fail, *proving* that the best solution so far was optimal (or, if no solution has been previously found, that there is no solution satisfying all the constraints). In order to quickly obtain solutions of good quality, which is mandatory in an operational real-time context, our search strategy first focus on maneuvers that least increase the cost.

V. RESULTS

The benchmark generation (section III-A) and the two conflict resolution algorithms (section IV) were implemented, using the FaCiLe constraint library [21] for the CP model. The following results were obtained on a standard workstation consisting of an octo-core Intel[®] Xeon[®] processor running at 3.4 GHz and equipped with 8 GB of memory.

A. Benchmark

A total of 120 instances were produced, based on situations with 5, 10, 15 and 20 aircraft in the same airspace volume and with uncertainty levels 1, 2 and 3 (see section III-A), thus changing the density of the problem. Ten random instances were created for each set of parameters, in order to assess the reliability of the resolution algorithms.

The generation of a given instance is highly parallelizable (the computation of the constraint between two given aircraft is independent from other constraints in the problem), which made it possible to dramatically reduce the needed computation time. As an example, the biggest and hardest instances (20 aircraft with high uncertainty level) were produced in less than three minutes while the smallest ones only needed a few seconds.

Figure 6 shows the influence of the number of processors used on the benchmark generation time for a given instance. The time saving is quite huge, since only 10 seconds are

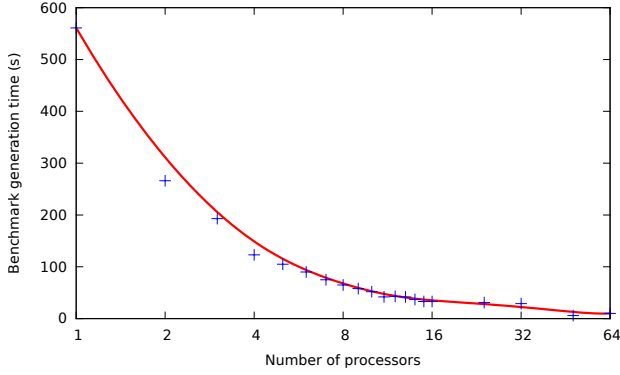


Fig. 6. Benchmark generation time w.r.t. number of processors. The horizontal scale is logarithmic.

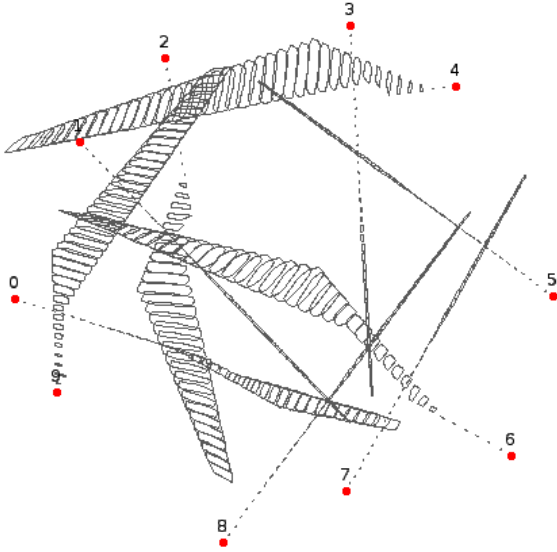


Fig. 7. A solution to a 10-aircraft conflict. Trajectories are depicted as sequences of convex hulls, representing the uncertainty.

necessary with 64 processors where it took more than 9 minutes to a single processor. However, the gain becomes less interesting when the number of processors further increases, because the communication overhead between processes then takes a significant amount of time. For the type of instances we generated, 16 processors seemed to constitute a fair compromise.

B. Conflict Resolution

The resolution algorithms were both limited to a 5 minutes execution time, in order to be compatible with the time constraints of an operational setting. In this context, all feasible instances were solved within seconds, and an optimality proof was obtained for most of them. Figure 7 shows a solution for a 10-aircraft conflict.

1) *Computing Times*: In more details, table I provides the computation times (averaged over the 10 different instances for each set of parameters) for finding the best solution. Instances with 5 and 10 aircraft are efficiently solved (under one second) by both algorithms (CP being a bit faster than EA). Most

TABLE I
AVERAGE TIME (IN SECONDS) FOR FINDING BEST SOLUTION WITH EA AND CP ALGORITHMS, FOR EACH SET OF PARAMETERS.

	n							
	5		10		15		20	
	CP	EA	CP	EA	CP	EA	CP	EA
ϵ_{low}	0.00	0.02	0.22	0.97	24.08	2.01	75.14	95.98
ϵ_{med}	0.00	0.02	0.27	1.44	45.17	32.60	79.61	184.61
ϵ_{high}	0.00	0.02	1.04	0.37	48.59	93.19	58.44	274.16

TABLE II
AVERAGE COST OF BEST SOLUTIONS FOR EACH SET OF PARAMETERS. RED CELLS INCLUDE SOLUTIONS THAT WERE NOT PROVED OPTIMAL, 2-IN-1 CELLS CORRESPOND TO SETS OF PARAMETERS WHERE BOTH CP AND EA REACHED OPTIMAL SOLUTION.

	n							
	5		10		15		20	
	CP	EA	CP	EA	CP	EA	CP	EA
ϵ_{low}	5.3		29.8		86.3	86.8	185.8	176.9
ϵ_{med}	4.2		46.6		104.0	104.0	267.6	282.8
ϵ_{high}	5.1		45.7		170.4	156.3	299.0	305.0

15-aircraft instances are solved within one minute, while 20-aircraft instances often need a few minutes. Moreover, a proof of optimality is obtained (with CP only) on all instances with 5 and 10 aircraft and almost all instances with 15 aircraft. When 20 aircraft are involved, however, optimality proof is not reached within the five minutes time limit.

Particularly interesting is the fact that, for instances that do not have any solution, a proof of non feasibility is obtained within one second. This could make it possible to generate, in a real-time setting, a new instance where, for the same situation, more maneuvers would be allowed, hopefully giving a resolution to the conflicting situation.

Finally, in almost all instances, including the toughest ones, a first solution was found within seconds. This means that in a real-time operational context, it could be possible to quickly provide the controllers with a first set of maneuvers that solves the conflict, so that it could be their choice to transmit them right away or wait for a more efficient solution, depending on their current workload and the urgency of the situation.

2) *Cost of Solutions*: Table II provides average costs for each set of parameters. According to the definition given in equation 2 (section III-B), each maneuver has a cost belonging to the interval $[0, 50]$ for the investigated instances. As expected, the cost increases with the number of aircraft involved, because the density of aircraft and conflicts increases with this parameter for a given constant airspace volume (cf. section III-A). The maneuver cost per aircraft varies from less than 1 for the smallest instances to 15 for the hardest ones.

Figure 8 depicts the cost of the best solution found with respect to the *intrinsic difficulty* ρ of the instance. The intrinsic difficulty is here defined as the total number of forbidden couples of maneuvers:

$$\rho = \sum_{\substack{i,j \in [1,n]^2 \\ i < j}} |c_{ij}|$$

where c_{ij} is the constraint between aircraft i and j , as defined in equation 4. Clearly, the cost of the best solutions is closely correlated to the intrinsic difficulty of the problem, which

could be used a priori to determine the expected efficiency of resolution.

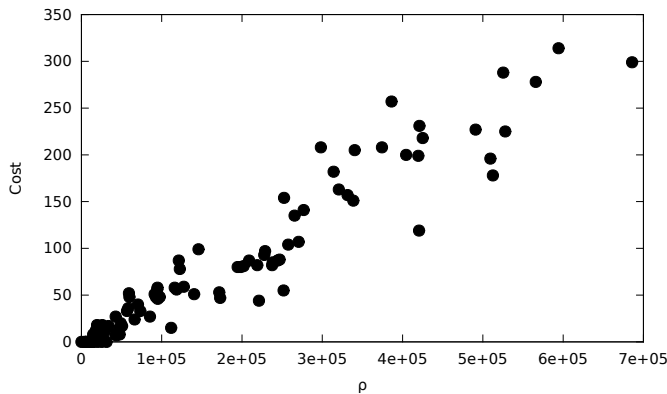


Fig. 8. Cost of the best solution found w.r.t. the intrinsic difficulty ρ of the instance.

In terms of cost, CP and EA are equivalently efficient: they both reach optimal solutions for almost all instances involving 15 or less aircraft, and alternately give the best solution for 20-aircraft instances. It would therefore be interesting to run both algorithms in parallel for a given instance, in order to always get the best possible solution.

VI. CONCLUSION AND FURTHER WORK

We have presented a new benchmark framework for the generation and solving of air traffic conflict resolution problems, with many configuration opportunities. Unlike other previous approaches, we have proposed to separate the generation of instances from their resolution, giving the possibility to easily test different algorithms for solution search and optimization.

The production of the benchmark is highly configurable: the density of the conflict (controlled by the number of aircraft involved or the volume of the considered airspace), the number of authorized maneuvers and the level of uncertainty to be taken into account are the main parameters, but the tuning can be even finer, e.g. with the possibility of defining custom maneuvers or trajectory uncertainties. The output is a data file containing all pre-computed trajectories and a list of maneuvers pairs that cannot be performed simultaneously. As this phase is highly parallelizable, this method can be used to generate an entire benchmark database within a reasonable computation time.

To illustrate the usefulness of our benchmark framework, we have also described two different approaches to solve the generated conflict problems, an Evolutionary Algorithm and a Constraint Program, and shown how to fairly compare their results on the 120 instances of various difficulties of our proposed benchmark basis. Most of these instances were solved in less than one second, the hardest ones needing a few minutes of computation. With the CP algorithm, optimality proofs were obtained in most cases, and instances without solution were proved inconsistent within one second. As expected, the cost of the solutions, i.e. the sum of maneuver costs defined in the conflict data, increases with the intrinsic

difficulty of the instance, defined as the overall amount of forbidden maneuver pairs.

We plan to extend our approach in order to consider vertical maneuvers, like a flight level change, interrupted climb or anticipated descent, thus increasing the configurability and generality of the framework. In terms of efficiency, the detection phase could be enhanced by the use of a fastest algorithm for computing distances between the convex hulls that model the uncertainties.

The realism of the instances can be greatly improved by integrating the conflict generation into our fast-time simulation platform CATS (or other third-party simulators), in order to extract the conflicting situations from the simulated traffic. This would also make it possible to test resolution algorithms in a fast-time simulation setting over a whole day of traffic.

Finally, we are currently working on yet other algorithms for the conflict resolution problem, such as an ad hoc *branch and bound* and a *Tabu Search*, and their hybridization in order to increase the efficiency and the robustness of the resolution.

REFERENCES

- [1] K. Zeghal, "Techniques réactives pour l'évitement," tech. rep., ONERA, June 1993.
- [2] D. Delahaye, C. Peyronne, M. Mongeau, and S. Puechmorel, "Aircraft conflict resolution by genetic algorithm and B-spline approximation," in *ENRI International Workshop on ATM/CNS*, (Tokyo, Japan), EIWAC, 2010.
- [3] L. Pallottino, E. Féron, and A. Bicchi, "Conflict resolution problems for air traffic management systems solved with mixed integer programming," *IEEE Transactions on Intelligent Transportation Systems*, vol. 3, no. 1, pp. 3–11, 2002.
- [4] A. Vela, S. Solak, W. Singhose, and J. Clarke, "A mixed integer program for flight-level assignment and speed control for conflict resolution," in *Proceedings of the Joint 48th IEEE Conference on Decision and Control and 28th Chinese Control Conference*, IEEE, 2009.
- [5] A. Alonso-Ayuso, L. Escudero, and F. Martin-Campo, "Collision avoidance in air traffic management: a mixed-integer linear optimization approach," *IEEE Transactions on Intelligent Transportation Systems*, vol. 12, no. 1, pp. 47–57, 2011.
- [6] D. Rey, C. Rapine, R. Fondacci, and N. E. Faouzi, "Minimization of potential air conflicts through speed regulation," *Transportation Research Record: Journal of the Transportation Research Board*, vol. 2300, pp. 59–67, 2012.
- [7] N. Durand, J.-M. Alliot, and J. Noailles, "Automatic aircraft conflict resolution using genetic algorithms," in *Proceedings of the Symposium on Applied Computing, Philadelphia*, ACM, 1996.
- [8] G. Granger, N. Durand, and J. Alliot, "Optimal resolution of en-route conflicts," in *4th ATM R&D Seminar*, 2001.
- [9] H. Erzberger, "Conflict probing and resolution in the presence of errors," in *Proceedings of the 1st USA/Europe ATM R&D Seminar*, 1997.
- [10] N. Durand and G. Granger, "A traffic complexity approach through cluster analysis," in *5th ATM R&D Seminar*, 2003.
- [11] Z. Michalewicz, *Genetic algorithms + Data Structures = Evolution Programs*. Springer-verlag, 1992.
- [12] P. Van Hentenryck, "Constraint solving for combinatorial search problems: a tutorial," in *Principle and Practice of Constraint Programming CP'95* (U. Montanari and F. Rossi, eds.), vol. 976 of *Lecture Notes in Computer Science*, (Cassis, France), pp. 564–587, Springer, September 1995.
- [13] N. Barnier and C. Allignol, "Trajectory deconfliction with constraint programming," *The Knowledge Engineering Review*, vol. 27, no. 03, pp. 291–307, 2012.
- [14] R. L. Graham, "An efficient algorithm for determining the convex hull of a finite planar set," in *Information Processing Letters*, 1992.
- [15] M. de Berg, M. van Kreveld, M. Overmars, and O. Schwarzkopf, *Computational Geometry – Algorithms and Applications*. Springer, second ed., 1998.
- [16] D. E. Goldberg, *Genetic Algorithms in Search, Optimization and Machine Learning*. Boston, MA, USA: Addison-Wesley Longman Publishing Co., Inc., 1989.

- [17] X. Yin and N. Germy, “A fast genetic algorithm with sharing scheme using cluster analysis methods in multimodal function optimization,” in *Proceedings of the Artificial Neural Nets and Genetic Algorithm International Conference* (R. F. Albrecht, C. R. Reeves, and N. C. Steele, eds.), (Innsbruck, Austria), Springer-Verlag, 1993.
- [18] J.-M. Alliot, H. Gruber, and M. Schoenauer, “Using genetic algorithms for solving ATC conflicts,” in *Proceedings of the Ninth Conference on Artificial Intelligence Application*, IEEE, 1993.
- [19] N. Durand, J.-M. Alliot, and J. Noailles, “Algorithmes génétiques : un croisement pour les problèmes partiellement séparables,” in *Proceedings of the Journées Évolution Artificielle Francophones*, EAF, 1994.
- [20] F. Boussemart, F. Hemery, C. Lecoutre, and L. Sais, “Boosting systematic search by weighting constraints,” in *European Conference on Artificial Intelligence - ECAI*, pp. 146–150, 2004.
- [21] N. Barnier and P. Brisset, “FaCiLe: a Functional Constraint Library,” in *Colloquium on Implementation of Constraint and Logic Programming Systems CICLOPS’01 (Workshop of CP’01)*, (Paphos, Cyprus), December 2001.

AUTHORS

Cyril Allignol is an assistant professor at École Nationale de l’Aviation Civile (ENAC). He graduated from ENAC as an engineer

in 2006, and received a PhD (2011) in computer science from the University of Toulouse.

Nicolas Barnier is an assistant professor at ENAC. He graduated from ENAC as an engineer in 1997, and received a PhD in computer science in 2002 from the University of Toulouse. He is one of the authors of FaCiLe, an open source Constraint Programming library for the functional language OCaml.

Nicolas Durand graduated from the École Polytechnique de Paris in 1990 and ENAC in 1992. He has been a design engineer at the Centre d’Études de la Navigation Aérienne (then DSNA/DTI R&D) since 1992, holds a PhD in Computer Science (1996) and got his HDR (French tenure) in 2004. He is currently professor at the ENAC/MAIAA lab.

Jean-Marc Alliot graduated from the École Polytechnique de Paris in 1986 and ENAC in 1988. He received a PhD in 1992 in Computer Science and got his HDR (French tenure) in 1996. He has been the head of LOG (Global Optimization Lab, ENAC/CENA) and then the head of DSNA/DTI R&D until 2011. He is currently research director at IRIT (Institut de Recherche en Informatique de Toulouse).